Title:

Experimental analysis of a microencapsulated PCM slurry as thermal storage system and as heat transfer fluid in laminar flow.

Authors:

Mónica Delgado*, Ana Lázaro, Javier Mazo, José María Marín, Belén Zalba

Aragón Institute for Engineering Research (I3A), Thermal Engineering and Energy Systems Group, University of Zaragoza
Agustín Betancourt Building, C/María de Luna 3, 50018 Zaragoza, Spain
Phone: (+34) 976761000 ext: 5258, Fax: (+34) 976762616

* Corresponding Author, monica@unizar.es

Abstract:

A microencapsulated PCM (Phase Change Material) slurry is a dispersion where the PCM, microencapsulated by a polymeric capsule, is dispersed in water. Compared to water, these new fluids have a higher heat capacity during the phase change and a possible enhancement, as a result of this phase change, in the heat transfer phenomenon. From the literature review, the existing experimental results are found incomplete and contradictory in many cases. For this reason the objective of this investigation is to analyze the heat transfer phenomenon in mPCM slurries, proposing a new methodology, developed by the authors. In this manner, an experimental analysis using a slurry with a 10% weight concentration of paraffin has been conducted to study it as a thermal storage material and as a heat transfer fluid. The results demonstrated an improvement of approximately 25% on the convective heat transfer coefficient when compared to water.

Keywords: Microencapsulated PCM slurry, Convective heat transfer, Thermal Energy Storage, Experimental, Laminar slurry flow

Nomenclature

c_p	specific heat capacity (kJ/(kg·K))
f	fraction of heat losses
h	enthalpy (kJ/kg)
I	current (A)
$\dot{m}$	mass flow rate (kg/s)
$\dot{Q}$	heating power absorbed or transported by the fluid (W)
T	temperature (ºC)
$\dot{W}$	pumping power (W)
ΔU	voltage (V)

Greek symbols:

α	convective heat transfer coefficient (W/(m²·K))
η	energy ratio

Subscripts:

in	inlet of the heat transfer section
m_1	melting beginning
m_2	melting final
out	outlet of the heat transfer section

Adimensional numbers

Gz	Graetz number
Nu	Nusselt number

Abbreviation

LHS	latent heat system

mPCM microencapsulated phase change material
PCM phase change material
TES thermal energy storage
vol volume

1. Introduction

One of the main contributions to the rational use of energy is provided by the Thermal Energy Storage (TES). These systems allow for the use of energies that provide unconstant supply throughout time, such as waste heat or renewable energies (solar energy, cold environment, etc). TES technique with PCMs attracted great interest in a large number of thermal applications. In the review by Zalba et al. [1], the authors listed materials used as PCM. They dealt with the heat transfer phenomenon and compiled the thermal applications found in literature. In recent years, a new technique has been proposed to use the phase change materials as pumpable heat transfer fluids and as heat storage systems. This new technique consists of microencapsulating the PCM and dispersing it in a fluid to form a microencapsulated PCM slurry (mPCM slurry). Zhang et al. [2] presented a literature review on phase change material slurries. One of the sections of this paper was focused on mPCM slurries, where the thermal properties, the fluid flow and the heat transfer characteristics for design and optimization of systems were considered.

MPCM slurries could present potential advantages when used as heat transfer fluids, such as (1) heat exchange at an approximately constant temperature, (2) higher heat transfer rate due to the thermal rise because the phase change, (3) higher heat transfer rate between the PCM microcapsules and the fluid due to the high ratio surface/volume of the PCM microcapsules, (4) lower pumping power as a consequence of the decrease in mass flow due to higher heat capacity, (5) possibility of using the same medium to carry and store energy, reducing the heat loss, as a second heat exchanger is not necessary. The possible improvement of the heat transfer process would allow for improvements in the performance of devices with different thermal levels, which constitute solar heating and cooling systems.

As a thermal storage material, mPCM slurries present high heat capacity during the phase change. Such higher thermal storage density makes the mPCM slurry systems advantageous against conventional systems of sensible storage in water, also being competitive against tanks with macroencapsulated PCM. Storage tanks would be simpler with the use of mPCM slurries, as there is no necessity for macroencapsulation. Besides the specific design issue of the latent heat system according to the geometry of the container, another issue identified is the low thermal conductivity of the PCM. The latter causes long response times, limiting the heat flow absorbed or released by the PCM. This issue was tentatively addressed by embedding structures with high thermal conductivity materials, by using finned heat exchangers, and by encapsulating the PCM into containers with high surface/volume ratios [3]. With mPCM slurry systems the response time could be shorter than using conventional latent heat systems. In this way, continuous operation could be guaranteed in solar cooling systems.

Huang et al. [4] listed the recommendable properties for a PCM slurry utilized in cold storage and distribution systems, specifically: the phase transformation range should match the designed operating temperature range, absence of subcooling, narrow phase temperature range, high heat

transfer rate, and small pressure drop in pump systems. Besides, the slurry should be stable during long-term storage and present reversible freezing/melting cycles under thermal-mechanical loads.

Although there are numerous presented advantages in the use of PCM slurries, there is a lack of technical experience. The main issues encountered as a thermal storage material are subcooling and the unstable processes presented by slurries. When used as heat transfer fluids, a higher heat transfer rate compared to water is interesting but existing studies, specially experimental studies, have not obtained clear conclusions. Regarding scientific literature, all numerical studies agree that the most influentional parameter is the Stefan number. Some studies also point out PCM concentration [5-8] and phase change temperature range [6, 8, 9] as relevant factors. However, more convincing conclusions cannot be drawn from these experimental results. Rao et al. [10] concluded that in low mass flow rates, PCM slurry presented a better cooling performance, and when the PCM concentration was increased, the convective heat transfer coefficient improved in comparison to water. Nevertheless, with higher mass flows, the cooling performance deteriorated. In the experimental study of Wang et al. [11], an improvement of the heat transfer coefficient was observed both under laminar and turbulent flow conditions. On the contrary, Alvarado et al. [12] obtained lower heat transfer coefficients in comparison to water, for the same velocities in his experimental investigation under turbulent conditions.

Another case of different results under similar studied conditions are the experimental works of Heinz and Streicher, and Diaconu et al. In the former [13], natural convection is compared to water in a tank with a typical spiral-type heat exchanger, using mPCM slurries with PCM concentration of 20, 30 and 40%, with a melting temperature of approximately 60ºC. In the latter [14], natural convection is compared to water in a tank with helically-coiled tube heat exchanger, using a mPCM slurry with a 45% PCM concentration and melting temperature range between approximately 4-7ºC. In the first case, the natural convection coefficient was worse for all PCM concentrations, and on the contrary, in the second case this coefficient improved significantly during the phase change interval when compared to water.

Analyzing the literature, information is available on the factors that influence the heat transfer phenomenon and how they interact, but the effects are not, for the moment, clear. For example, PCM concentration has several opposite effects on heat transfer. On one hand, an increase in PCM concentration results in an increase of heat capacity and therefore reductions in the slurry and wall temperatures. On the other hand however, such an increase also results in an increase of viscosity (equivalent to a decrease of the turbulence degree) and a reduction of thermal conductivity, deteriorating the heat transfer coefficient.

The objective of this investigation is to analyze the heat transfer phenomenon in mPCM slurries, as existing results are incomplete and conflictive in many cases. Existing studies neither present clear evidence on the improvement of heat transfer, nor how relevant factors are related to a possible increase in heat transfer coefficients. This paper designs an experimental installation to study the convective heat transfer in a circular duct under constant heat flux and laminar flow conditions. For this, it proposed an appropriate test methodology for the determination of these convective coefficients, as the variation observed in the experimental results up to the moment, may come from using an unsuitable methodology.

2. Thermal properties of the mPCM slurry

The analyzed mPCM slurry consists of microcapsules of paraffin coated by a polymer and dispersed in water through detergents. The weight concentration of the PCM microcapsules is approximately of 10%. This mPCM slurry has been purchased in the commercial market. The phase change temperature range and the phase change enthalpy as a function of the temperature were obtained with a T-history method installation. When a material is being characterized, the sample must be representative of the material that is investigated. In this case, the PCM slurry is constituted of different substances. The volume of the sample should be of at least a few cm^3 or more if possible [15], to assure that the sample has the correct chemical and physical composition that is representative of the bulk material. For this reason, an installation of the T-history method was used to determine the Enthalpy-Temperature curve during the phase change of the mPCM slurry. The basic aspects of the operation principle of this method proposed by Zhang et al. [16] are: one-dimensional heat transfer: in the radial direction; the systems formed by the container, the reference substance and the PCM respectively, are systems of capacity; heat transfer from the containers of the reference and PCM to the air of the chamber is by natural convection. In this way, the experiment proposed by Zhang, entails recording the chamber temperature and the temperatures during the phase change of the PCM, inside of two equal tubes that contain respectively the substance that change the phase and the substance of reference, whose specific heat is known. After obtaining the temperature-time curves of the PCM and of the reference, these data can be treated to estimate the themophysical properties. Figure 1 shows the Enthalpy-Temperature curve of the mPCM slurry compared to water, obtained with an installation of the T-history method. The phase change temperature range of the mPCM slurry was of approximately 25.5-28ºC and the phase change enthalpy for this range was of approximately 20 kJ/kg. The particle size distribution was of approximately 1-20 µm. Hysteresis and subcooling phenomena were not observed when comparing the solidification and melting curves.

3. Experimental setup

A flow loop was designed and built to study both flow and heat transfer characteristics of the mPCM slurry. The experimental setup was designed to measure the convective heat transfer and the pressure drop of the mPCM slurry flowing through a circular tube. Specifically, the experimental setup allows for obtaining local convective heat transfer coefficients under constant heat flux in a tube. The calculation of these coefficients requires the registration of the heat flux absorbed by the tube, of the fluid temperature and of the wall temperature along several locations. Figure 2 shows the schematic diagram of the experimental setup, which consists of a thermostatic bath, a Coriolis flow meter, a hydrodynamic entry section, a heat transfer section, a pump and control valves. The mPCM slurry is pumped from the thermostatic bath and flows through the loop. The slurry enters the hydrodynamic section and proceeds to the heat transfer section, where heating wires provide uniformly-distributed heat flux. Leaving the heat transfer section, the mPCM slurry returns to the thermostatic bath for cooling, passing through a thermal equilibrium section. The mass flow is measured by a Coriolis flow meter and controlled by control valves. Table I shows the characteristics of the different devices in the experimental installation and the magnitudes measured and controlled in the experiments.

The heat transfer section consists of a 10 mm copper tube with 1.82 m length. After the length of the heat transfer section was established, the power of the heating wires that guaranteed the corresponding phase change was taken into account. The hydrodynamic entry section has sufficient length to assure that the flow at the entrance of the heating section is fully hydrodynamically developed. The length of the hydrodynamic entry region was calculated with Fluent, taking into account the dimensions and geometry of the experimental installation. The hydrodynamic entry region measures approximately 1.5 m.

The thermostatic bath has a centrifugal pump, chosen in accordance with the work of Gschwander et al. [17]. After testing different pumps, Gschwander et al. concluded that centrifugal pumps were able to pump the mPCM slurry during a longer period of time without self-destruction or damage to the microcapsule shells. The choice of a Coriolis flow meter is appropriate considering the characteristics of the flow to be measured.

Eleven type T thermocouples were placed to measure the wall temperature, and two Pt100 were chosen to measure the fluid temperature at the inlet and at the outlet of the heat transfer section. Due to the impossibility of installing sensors along the heat transfer section, the temperatures of the fluid along the tube will be calculated.

Ten isolated nichrome wires, connected in parallel, were coiled around the copper tube to heat the section. These heating wires were connected to the 230 V AC power supply through a phase angle electronic regulator, which varied the voltage and therefore varied the heating power provided to the heat transfer section. The maximum heating power was 3600 W when the heating wires were connected to 230 V. The heat flux provided to the heat transfer section must guarantee complete phase change of the dispersed PCM, so that the difference between inlet and the outlet temperatures is noticeable and higher than the Pt100 uncertainty. The current and the voltage were measured by an ammeter and a voltmeter, respectively. Heat losses were minimal, approximately 3%, and therefore the heat transfer section was not thermally isolated. The heat losses were taken into account during data processing.

A pressure differential transducer has been chosen to measure the pressure drop in the heat transfer section. All measured data was recorded by a HP-34970A Data Logger.

4. Experimental setup validation

Validation of the experimental setup was accomplished by testing the setup with water and comparing the results with theoretical values. Pressure drop, heat flux and wall temperature measurements were successfully validated.

The pressure drop tests were carried out at different fluid temperatures and with different mass flows. Water pressure drop data were recorded and compared to the values obtained with the Darcy-Weisbach equation and the steady-flow energy equation. The friction value for laminar flow conditions was calculated with the Hagen Poiseuille equation and, for turbulent flow conditions, (Reynolds number from 3000 to 20000) the Blasius equation was utilized. Measured values fit well with the theoretical values, with an error lower than 3%.

The energy balance equation (eq. 1) was used to obtain the heat flux. The measurement of the fluid temperature at the inlet and outlet of the heat transfer section is determinant, as the ammeter and voltmeter only indicate the heating power of the wires, not the heating power absorbed by the fluid. In this installation, the length of the thermal entry region in the case of laminar flow is higher than the length of the heat transfer section (for water under laminar flow conditions, in the most unfavorable conditions, the thermal entry length would measure approximately 5 m). Therefore the temperature at the outlet of the thermal equilibrium section was taken as the outlet fluid temperature (the thermal equilibrium section was placed after the heat transfer section). A greater degree of mixing is caused by the length of thermal entry region and by elbows, therefore the profile of temperatures is uniform throughout the cross section.

$$\dot{Q} = \dot{m} \cdot C_p \cdot (T_{out} - T_{in}) \quad (1)$$

When the wall temperatures were checked, in certain conditions, the measured wall temperature showed good agreement with the theoretical wall temperature (errors below 5% in the Celsius scale), while in other conditions this error could reach 15%. The theoretical wall temperatures were calculated through the Kays correlation (eq. 2) for the thermal entry region [18]:

$$Nu = 4.36 + \frac{0.023 * Gz_X}{1 + 0.0012 * Gz_X} \quad (2)$$

In theses cases, the establishment of a correction model for the wall temperatures is necessary. Goel et al. [19] used a correction model in his experimental work, as differences were observed between the experimental wall temperatures and those obtained by the analytical solution. If the error correction was not used, the results were more optimistic.

In the current experimental analysis, these differences could be mainly caused by three reasons:

1) Interruption of the heat flux for the placement of a thermocouple is necessary. The difference between the wall temperature calculated with the Kays correlation (2) and the measured wall temperature will depend on the axial and radial thermal resistance, therefore depending on the convective heat transfer coefficient.
2) Possible influence of the heat flux on the thermocouple (possible increase in temperature).
3) Heat losses from the thermocouple to the ambient.

In other studies the analyzed phenomenon was well understood, and a functional form could be proposed through theoretical considerations. In this case, the factors causing the errors could be assumed. Nevertheless, the proposition of an accurate model to describe this process is difficult. Under these circumstances, an empirical model can be useful. To such end, a difference between the calculated wall temperature and the measured wall temperature was obtained for every temperature sensor using the least squares fitting. The convective heat transfer coefficient must be known a priori and set as the objective value in order to calculate the error. Different values of α were tested to obtain this coefficient, resulting in different correction values. If the result of the application of a correction value on the wall temperature resulted in the tested α, the correction

was considered adequate. In figure 3, the algorithm of the correction model is shown. The values tested with water to obtain the correction model were within the value range to be tested with the mPCM slurry.

5. Experimental results

Firstly, the energy balance (eq. 3) must be verified in order to assure that the microcapsules do not adhere to any part of the experimental setup. If the mPCM slurry is not stable and homogeneous, the microcapsules could deposit in the different devices of the experimental installation. Gschwander and Schossig pointed out the danger of obstruction in small channels and tubes due to this phenomenon [20]. Thermal equilibrium between microcapsules and water was assumed.

$$(1-f)\cdot\Delta U\cdot I = h[T_{out}] - h[T_{in}] \quad (3)$$

The verification tests were performed for different mass flows and heat fluxes. Figure 4 shows the Enthalpy-Temperature curve obtained through the energy balance equation (along with its fitting to a sigmoidal curve) and its comparison with the Enthalpy-Temperature curve obtained previously with the T-history installation. A good agreement between the curves was observed, as the average difference between curves was of approximately 9% during the phase change range. It can be considered that there was no deposition or obstruction caused by the PCM microcapsules.

In the experimental work of Goel et al. [19] it was observed that the slurry of microencapsulated n-eicosane studied presented subcooling during the solidification process. The considerable differences between numerical and experimental results were attributed to this phenomenon. Due to subcooling, the PCM inside the microcapsules could not be in a complete solid phase when the slurry was about to enter the heat transfer section. Thus, the amount of absorbed heat by the microcapsules will be lower. With the mPCM slurry studied this issue did not occur as no subcooling was present, as shown in figure 1.

To sum up, the novelty of the present experimental method to analyze the heat transfer phenomenon is, that it takes into account the subcooling phenomenon, that PCM microcapsules may have deposited in the installation, and considers a correction model for the measurement of the wall temperatures. These three phenomena have to be taken into account, as if they are ignored in the treatment of the data, it can cause wrong results. This may be one of the reasons of such disparity of experimental results, obtained up to the moment. If the mPCM slurries were analysed according to this proposed methodology, the possible improvement or not of the heat transfer phenomenon would be able to be known with a higher certainty.

5.1 As a thermal storage fluid compared to water

The energy density was evaluated from the results obtained with the T-history installation in order to start the analysis of the mPCM slurry as a thermal storage material. Figure 5 shows the energy density for five different heat storage systems with a temperature gradient of 5ºC: a sensible heat storage system with water, three latent heat storage systems with the studied PCM slurry with 10, 30 and 50% concentration, and a typical latent heat storage system with a macroencapsulated

PCM filling 60% of the storage system volume. As was stated in the introduction, the higher thermal storage density of PCM slurries allows for a latent heat system with this fluid to be advantageous compared to a sensible heat system with water and competitive against a conventional latent heat system with PCM macroencapsulated in containers.

5.2 As a heat transfer fluid compared to water

For the analysis of the mPCM slurry as a heat transfer fluid, the pressure drop in the heat transfer section was measured and the Transported Thermal Energy vs. Pumping power compared to water was evaluated. The following energy ratio of improvement was defined (eq. 4) for this comparison:

$$\eta = \frac{\dot{Q}_{mPCMslurry} / \dot{W}_{mPCMslurry}}{\dot{Q}_{water} / \dot{W}_{water}} \quad (4)$$

Figure 6 presents the aforementioned defined ratio, obtained for different average fluid velocities. The energy ratio is higher for the mPCM in comparison to water when the fluid velocity is higher than 0.4 m/s. In figure 7 it can be observed that for the same transported thermal energy, the pumping power is lower for the mPCM.

Mass flows, heating powers and inlet fluid temperatures of the heat transfer section were varied in order to measure the wall temperatures. Table 2 shows data and main characteristics regarding the analyzed mPCM slurry, the geometry of the installation, and the boundary and test conditions. The correction model was applied to the measured wall temperatures with further comparison of these values with the calculated values for the case of water (obtained through Kays correlation (eq. 2)). The results showed a significant decrease in the wall temperature compared to water, resulting in a better cooling performance (figure 8). Dependence of the mass flow and the operation temperature range on the decrease of the wall temperature was also studied.

An “Operation temperature range” parameter was defined for the analysis, according to equation 5. This parameter shows if the phase change is in accordance with the heat transfer section. A parameter equal to 1 would mean that the mPCM slurry starts melting just as it enters the heat transfer section, and leaves the heat transfer section only when the PCM microcapsules are completely melted. A parameter under 1 would mean that the PCM microcapsules did not completely melt in the heat transfer section, and a parameter above 1 means that both liquid and phase change regions coexist in the heat transfer section. The parameter was defined taking into account the phase change and liquid regions, attributing in this way, different phenomena to each region.

$$\text{Operation temperatures range} = \frac{h[T_{out}] - h[T_{m1}]}{h[T_{m2}] - h[T_{m1}]} \quad (5)$$

As it was expected, when the phase change took place in the heat transfer section, the decrease of the wall temperature was more pronounced. In this manner, from an application viewpoint, it is interesting that the phase change temperature range fit the operation temperature range as much as possible. In figure 9 it can be observed that when the PCM has not completely melted in the heat transfer section, the reduction in the wall temperature is lower. The dependence of the decrease in wall temperature with the parameter “Operation temperature ranges” tends to be linear. Regarding mass flow, no clear evidence was found.

Figure 10 shows the convective heat transfer coefficients. If the mPCM slurry inlet temperature at the heat transfer section was lower than 24ºC (lower than the melting temperature), a first region where the heat transfer coefficient was lower compared to water was observed in Figure 10, as phase change had not started and the thermal conductivity of the mPCM slurry was lower than the thermal conductivity of the water. Consequently, it must be emphasized again that the slurry must enter the heat transfer section only when the PCM is starting to melt and the phase change region must fit the heat transfer section.

Figure 11 studies the phenomena influencing the improvement of the heat transfer process. It can be observed that the wall temperature decreased in consequence of a decrease of the fluid temperature due to phase change. However, the decrease in wall temperature is significant, approximately two times higher than the fluid temperature drop. Such significant decrease could be caused by different factors. Kasza and Chen described the improvement mechanisms related to heat transfer. Reviewed literature showed that an improvement of heat transfer takes place with or without phase change, because of the microconvection of particles [21].

The experimental results obtained according to the proposed methodology show a decrease of the wall temperature of the tube regarding to the water, as consequence of the decrease of the mPCM slurry temperature during the phase change. In addition to the higher heat capacity, this wall temperature decreases due to the microconvection phenomenon of the microcapsules, improving the heat transfer phenomenon and obtaining higher convective coefficients. Also, it is vital that the phase change temperature of the slurry fits with the operation temperatures range of the application in order to take advantage. To complete the study here analysed, as future work, the mPCM slurry must be analyzed for various concentrations, and to analyze in this way, this effect in the heat transfer phenomenon.

6. Conclusions

Existing experimental results obtained up to the moment are found incomplete and opposed in many cases and for this reason a new methodology to study the heat transfer phenomenon in Mpcm slurries has been proposed. The experimental results demonstrated that the investigated mPCM slurry could provide considerable advantages for thermal storage systems as well as heat transfer applications. The energy stored in the phase change temperature range was 75% higher than the stored energy in the same temperature range with water. In terms of heat transfer fluid, the mPCM had a higher ratio of Transported Thermal Energy to Pumping Power than that of water for fluid velocities over 0,4 m/s. Wall temperatures were lower for mPCM than water due to the phase change process, and local convective heat transfer coefficients were approximately 25% higher because of non-quantified phenomena. The phase change process must be adjusted to the heat transfer section in order to take advantage of any improvements that mPCM might

have over plain water. Regarding applications, the phase change temperature range will have to fit with the operation temperature range.

Acknowledgments

The present work was partially funded by the Spanish Government within the framework of research project ENE2008-06687-C02-02. The authors would like to acknowledge the participation and support of Compañía Industrial de Aplicaciones Térmicas S.A. –CIATESA-, a CIAT Group member, through the SOLTES project, partially funded by the Andalusian Innovation Agency IDEA and the Spanish CDTI.

References

[1] B. Zalba, J.M. Marín, L.F. Cabeza, H. Mehling, Review on thermal energy storage with phase change: materials, heat transfer analysis and applications, Appl. Therm. Eng. 23 (3) (2003) 251-283.

[2] P. Zhang, Z.W. Ma, R.Z. Wang, An overview of phase change material slurries: MPCS and CHS, Renew. Sustain. Energy Rev. 14 (2) (2010) 598-614.

[3] B. M. Diaconu, Transient thermal response of a PCS heat storage system, Energy Build. 41 (2) (2009) 212-219.

[4] L. Huang, M. Petermann, C. Doetsch, Evaluation of paraffin/water emulsion as a phase change slurry for cooling applications, Energy. 34 (9) (2009) 1145-1155.

[5] P. Charunyakorn, S. Sengupta, S.K. Roy, Forced convection heat transfer in microencapsulated phase change material slurries: flow in circular ducts, Int. J. Heat Mass Transf. 34 (3) (1991) 819-833.

[6] X. Hu, Y. Zhang, Novel insight and numerical analysis of convective heat transfer enhancement with microencapsulated phase change material slurries: laminar flow in a circular tube with constant heat flux. Int. J. Heat Mass Transf. 45 (15) (2002) 3163-3172.

[7] S. K. Roy, B. L. Avanic, Turbulent heat transfer with phase change material suspensions, Int. J. of Heat Mass Transf. 44 (12) (2001) 2277-2285.

[8] R. Zeng, X. Wang, B. Chen, Y. Zhang, J. Niu, X. Wang, H. Di, Heat transfer characteristics of microencapsulated phase change material slurry in laminar flow under constant heat flux, Appl. Energy. 86 (12) (2009) 2661-2670.

[9] R. Sabbah, M. M. Farid, S. Al-Hallaj, Micro-channel heat sink with slurry of water with micro-encapsulated phase change material: 3D-numerical study, Appl. Therm. Eng. 29 (2-3) (2009) 445-454.

[10] Y. Rao, F. Dammel, P. Stephan, G. Lin, Convective heat transfer characteristics of microencapsulated phase change material suspensions in minichannels, Heat Mass Transf. 44 (2) (2007) 175-186.

[11] X. Wang, J. Niu, Y. Li, X. Wang, B. Chen, R. Zeng, Q. Song, Y. Zhang, Flow and heat transfer behaviors of phase change material slurries in a horizontal circular tube, Int. J. Heat Mass Transf. 50 (13-14) (2007) 2480-2491.

[12] J. L. Alvarado, C. Marsh, C. Sohn, G. Phetteplace, T. Newell, Thermal performance of microencapsulated phase change material slurry in turbulent flow under constant heat flux, Int. J. of Heat Mass Transf. 50 (9-10) (2007) 1938-1952.

[13] A. Heinz, W. Streicher, Application of phase change materials and PCM-slurries for thermal energy storage, The Tenth International Conference on Thermal Energy Storage, Ecostock, New Jersey, May 31- June 2, 2006.

[14] B. M. Diaconu, S. Varga, A. C. Oliveira, Experimental assessment of heat storage properties and heat transfer characteristics of a phase change material slurry for air conditioning applications, Appl. Energy. 87 (2) (2010) 620-628.

[15] A. Lázaro, E. Günther, H. Mehling, S. Hiebler, J.M. Marín, B. Zalba, Verification of a T-history installation to measure enthalpy versus temperature curves of phase change materials. Meas. Sci. Technol. 17 (8) (2006) 2168-2174.

[16] Y. Zhang, Y. Jiang, Y. Jiang, A simple method, the T-history method, of determining the heat of fusion, specific heat and thermal conductivity of phase-change materials. Meas. Sci. Technol. 10 (3) (1999) 201-205

[17] S. Gschwander, P. Schossig, H. Henning, Micro-encapsulated paraffin in phase-change slurries, Sol. Energy Mater. Sol. Cells. 89 (2-3) (2005) 307-315.

[18] W. M. Kays, Numerical Solutions for Laminar-Flow Heat Transfer in Circular Tubes, Trans. ASME 77, (1955) 1265-1274.

[19] M. Goel, S. K. Roy, S. Sengupta, Laminar forced convection heat transfer in microcapsulated phase change material suspensions, Int. J. Heat Mass Transf. 37 (4) (1994) 593-604.

[20] S. Gschwander, P. Schossig, Phase Change Slurries as heat transfer and storage fluids for cooling applications, The Tenth International Conference on Thermal Energy Storage, Ecostock, New Jersey, May 31- June 2, 2006.

[21] K. E. Kasza, M. M. Chen, Improvement of the performance of solar energy or waste heat utilization systems by using phase-change slurry as an enhanced heat-transfer storage fluid, J. Sol. Energy Eng. 107 (1985) 229-236.

Figures and tables captions

Figure 8. Comparison of the wall temperature against water. Inlet temperature of the heat transfer section approx. 25ºC. Top image, mass flow~19 kg/h; Middle image, mass flow~37 kg/h; Bottom image, mass flow~50 kg/h.
Figure 9. Dependence of the operation temperatures range and of the mass flow on the decrease of wall temperature. Top image, Inlet temperature~24ºC; Middle image, Inlet temperature~25ºC; Bottom image, Inlet temperature~26ºC. LEGEND: Circles: Recorded values; Crosses: Projection of the recorded values on the plane Wall temperature decrease-Operation temperatures range.
Figure 10. Convective heat transfer coefficients compared to water. Mass flow~50 kg/h. Top image, Inlet temperature~24ºC; Middle image, Inlet temperature~25ºC; Bottom image, Inlet temperature~26ºC. Improvement of α (%) in the phase change region.
Figure 11. Influence of the decrease in fluid temperature on the decrease of wall temperature. Mass flow~19 kg/h. Inlet temperature~25ºC. Q=140 W.
Table 1. Magnitudes controlled and measured in the experimental installation and corresponding values.
Table 2. Data and characteristics of the tests carried out.

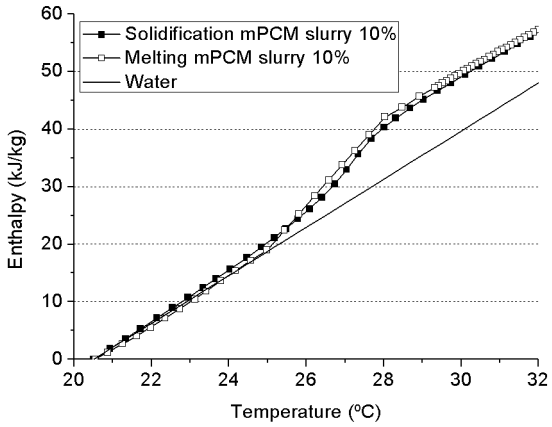

Figure 1.

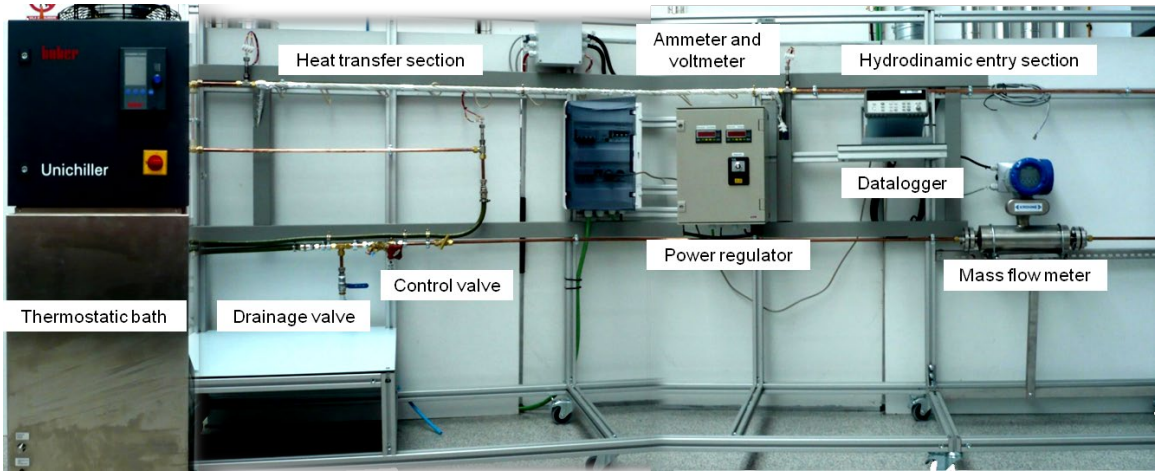

Figure 2.

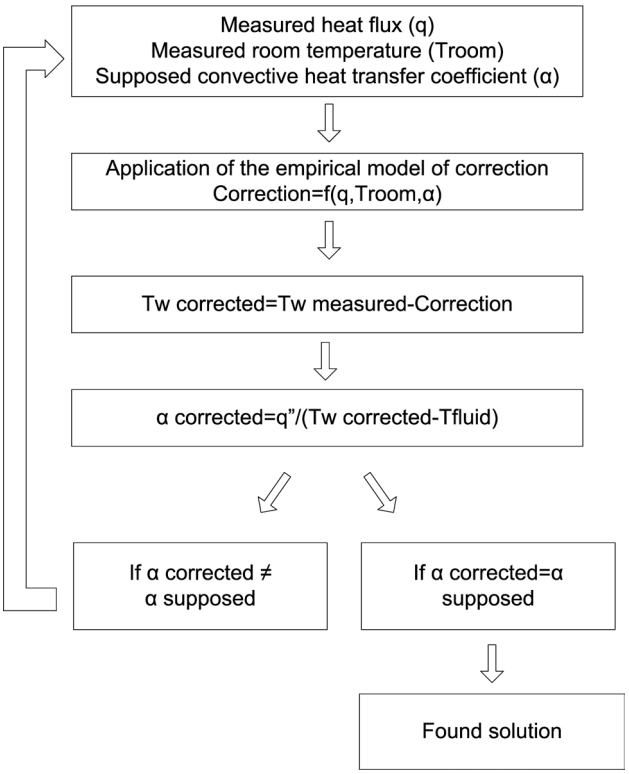

Figure 3.

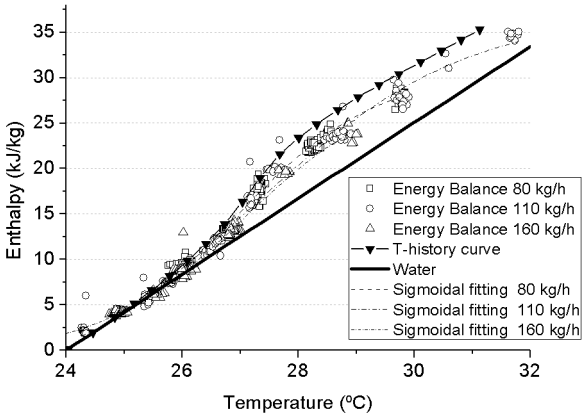

Figure 4.

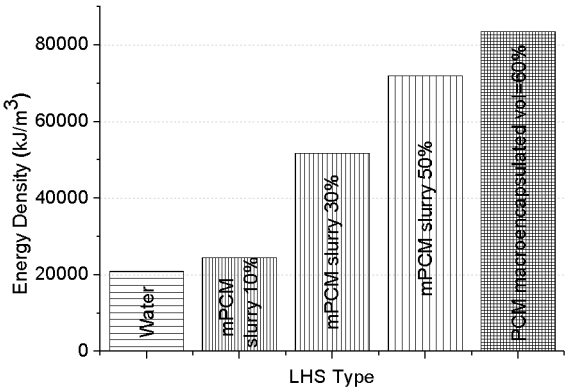

Figure 5.

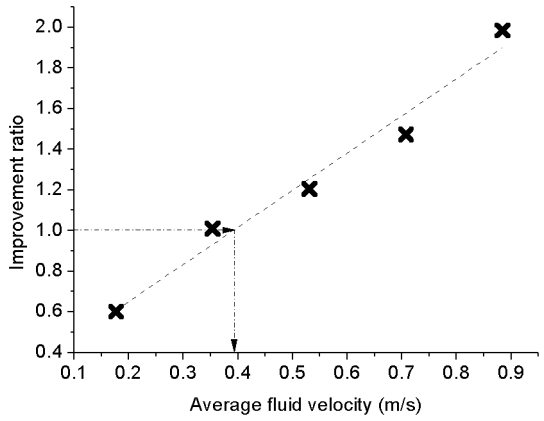

Figure 6.

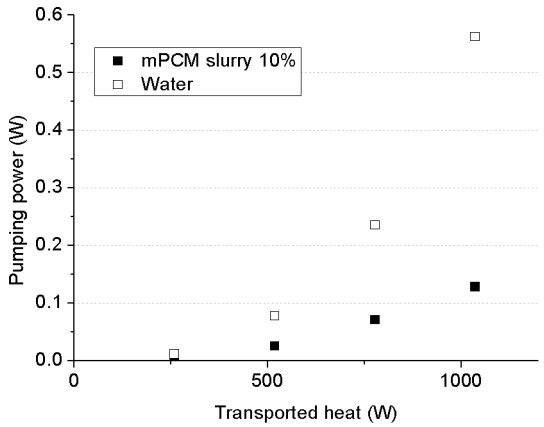

Figure 7.

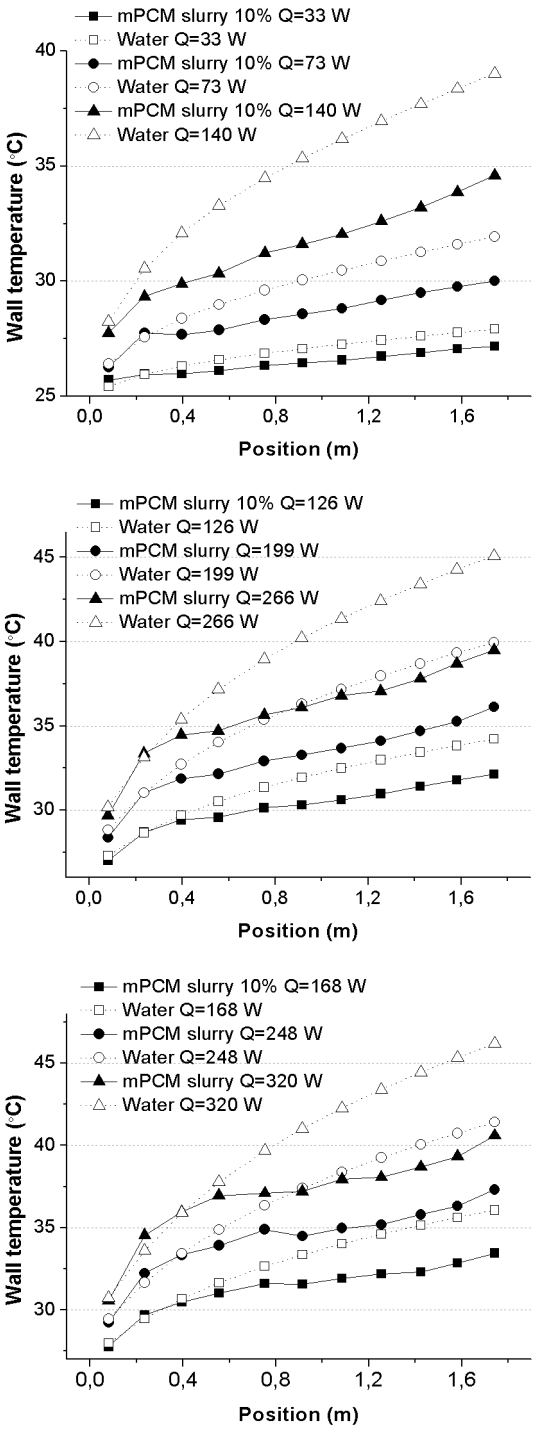
mPCM slurry 10% Q=33 W
Water Q=33 W
mPCM slurry 10% Q=73 W
Water Q=73 W
mPCM slurry 10% Q=140 W
Water Q=140 W
Wall temperature (°C)
Position (m)
mPCM slurry 10% Q=126 W
Water Q=126 W
mPCM slurry Q=199 W
Water Q=199 W
mPCM slurry Q=266 W
Water Q=266 W
Wall temperature (°C)
Position (m)
mPCM slurry 10% Q=168 W
Water Q=168 W
mPCM slurry Q=248 W
Water Q=248 W
mPCM slurry Q=320 W
Water Q=320 W
Wall temperature (°C)
Position (m)

Figure 8.

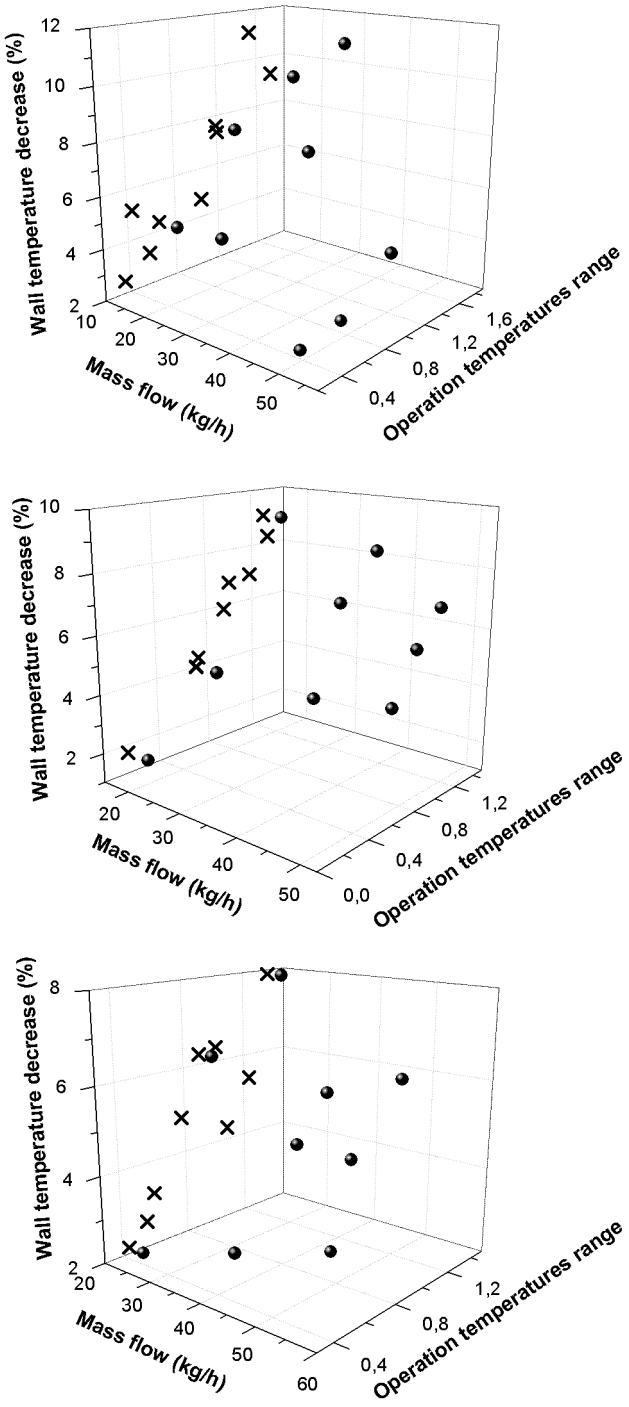
Wall temperature decrease (%)
12
10
8
6
4
2
10
20
30
40
50
Mass flow (kg/h)
0,4
0,8
1,2
1,6
Operation temperatures range
Wall temperature decrease (%)
10
8
6
4
2
20
30
40
50
Mass flow (kg/h)
0,0
0,4
0,8
1,2
Operation temperatures range
Wall temperature decrease (%)
8
6
4
2
20
30
40
50
60
Mass flow (kg/h)
0,4
0,8
1,2
Operation temperatures range

Figure 9.

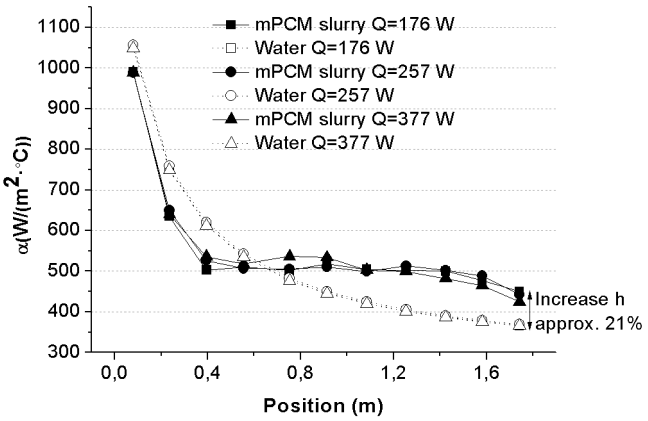
mPCM slurry Q=176 W
Water Q=176 W
mPCM slurry Q=257 W
Water Q=257 W
mPCM slurry Q=377 W
Water Q=377 W
Increase h
approx. 21%
α(W/(m2·°C))
Position (m)

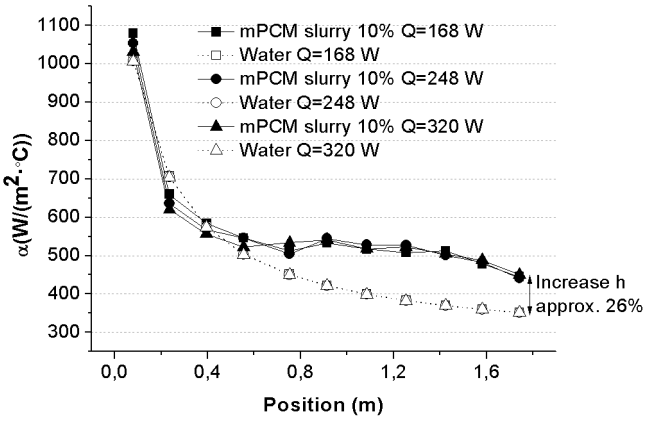
mPCM slurry 10% Q=168 W
Water Q=168 W
mPCM slurry 10% Q=248 W
Water Q=248 W
mPCM slurry 10% Q=320 W
Water Q=320 W
Increase h
approx. 26%
α(W/(m2·°C))
Position (m)

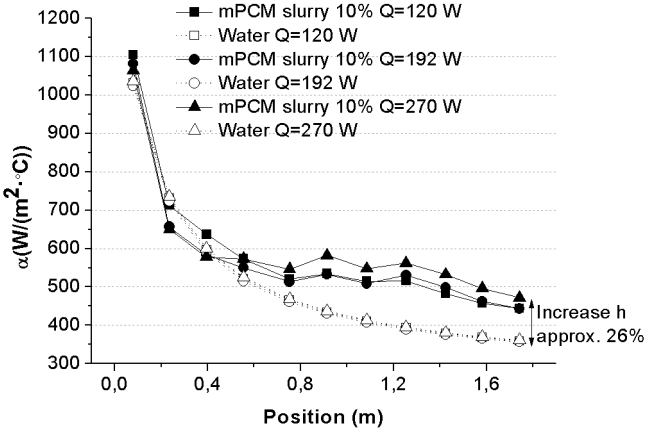
mPCM slurry 10% Q=120 W
Water Q=120 W
mPCM slurry 10% Q=192 W
Water Q=192 W
mPCM slurry 10% Q=270 W
Water Q=270 W
Increase h
approx. 26%
α(W/(m2·°C))
Position (m)

Figure 10.

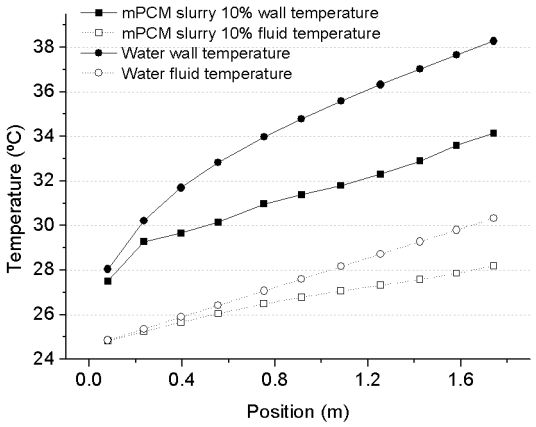
mPCM slurry 10% wall temperature
mPCM slurry 10% fluid temperature
Water wall temperature
Water fluid temperature
Temperature (ºC)
Position (m)
24
26
28
30
32
34
36
38
0.0
0.4
0.8
1.2
1.6

Figure 11.

	Magnitude	Equipment	Equipment characteristics	Measurement range
Controlled	mPCM slurry temperature (at the inlet of the heat transfer section)	Thermostatic bath	Centrifugal pump Stabilitiy: 0.1 K	
	Mass flow	Control valves		
	Heat flux	Isolated nichrome wires + Phase angle electronic regulator	Maximun heating power: 3600 W conected to 230 V	
Measured	Mass flow	Coriolis flowmeter	Accuracy: 0.2%	0-300 kg/h
	mPCM slurry temperature (at the inlet and outlet of the heat transfer section)	Pt 100 (4 wires)	Accuracy: +/- 0.15ºC	-
	Wall temperatures	Thermocouples type T	Accuracy: +/- 0.5ºC	-
	Heat flux	Ammeter and voltmeter	Accuracy: 1%	0-25 A; 0-230 V
	Pressure drop	Pressure differential transducer	Accuracy: 0.5%	0-0.16 bar

Table 1.

Mpcm slurry	-paraffin slurry -diameter distribution: 1-20 micrometer -PCM microcapsules concentration=10%
Geometry	-Circular tube -Lenght=1.82 m -Diameter=10 mm -Fully hydrodinamic developed section
Boundary conditions	-Constant heat flux
Test conditions	-Mass flow range: 20-50 kg/h (Laminar flow conditions) -Heating power range:30-400 W

Table 2.